



## Protein surface engineering and interaction studies of maltogenic amylase towards improved enzyme immobilisation

Nardiah Rizwana Jaafar<sup>a</sup>, Nashriq Jailani<sup>a</sup>, Roshanida A. Rahman<sup>a</sup>, Ebru Toksoy Öner<sup>b</sup>, Abdul Munir Abdul Murad<sup>c</sup>, Rosli Md Illias<sup>a,\*</sup>

<sup>a</sup> School of Chemical and Energy Engineering, Faculty of Engineering, Universiti Teknologi Malaysia, 81310 Skudai, Johor, Malaysia

<sup>b</sup> IBSB, Department of Bioengineering, Marmara University, Istanbul, Turkey

<sup>c</sup> Department of Biological Sciences and Biotechnology, Faculty of Science and Technology, Universiti Kebangsaan Malaysia, 43600 Bangi, Selangor Darul Ehsan, Malaysia

### ARTICLE INFO

#### Keywords:

Computational analysis  
Protein engineering  
Enzyme immobilisation  
Protein orientation  
Protein secondary structure

### ABSTRACT

A combined strategy of computational, protein engineering and cross-linked enzyme aggregates (CLEAs) approaches was performed on *Bacillus lehensis* G1 maltogenic amylase (Mag1) to investigate the preferred amino acids and orientation of the cross-linker in constructing stable and efficient biocatalyst. From the computational analysis, Mag1 exhibited the highest binding affinity towards chitosan (−7.5 kcal/mol) and favours having interactions with aspartic acid whereas glutaraldehyde was the least favoured (−3.4 kcal/mol) and has preferences for lysine. A total of eight Mag1 variants were constructed with either Asp or Lys substitutions on different secondary structures surface. Mutant Mag1-mDh exhibited the highest recovery activity (82.3%) in comparison to other Mag1 variants. Mutants-CLEAs exhibited higher thermal stability (20–30% activity) at 80 °C whilst Mag1-CLEAs could only retain 9% of activity at the same temperature. Reusability analysis revealed that mutants-CLEAs can be recovered up to 8 cycles whereas Mag1-CLEAs activity could only be retained for up to 6 cycles. Thus, it is evident that amino acids on the enzyme's surface play a crucial role in the construction of highly stable, efficient and recyclable CLEAs. This demonstrates the necessity to determine the preferential amino acid by the cross-linkers in advance to facilitate CLEAs immobilisation for designing efficient biocatalysts.

### 1. Introduction

Biocatalysts provide immense advantages to numerous industrial bioprocesses due to their high activity, high specificity and selectivity under mild reaction conditions. Furthermore, the use of enzymes in industrial applications has been widely touted as ‘green’ technology as it is a sustainable alternative to classical chemical catalysis and do not possess any environmentally hazardous attributes thus providing an ‘eco-friendly’ solutions or environment [1,2]. However, free or naturally occurring enzymes are generally not suited for many important industrial catalytic processes owing to the disparity between their native physiological conditions and the manufacturing environment as well as the lack of recovery of the biocatalysts during downstream processes [3,4]. Approaches including addition of ligands/additives, chemical modification, protein engineering and enzyme immobilisation have been utilised to tackle these limitations.

Enzyme immobilisation technology has leverage over the use of free

enzymes. It enhances the enzymological attributes including catalytic activity, specificity and stability towards a broad range of temperatures, solvents and pHs, as well as recyclability [5–7]. Its ability to be separated and recovered from the reaction mixture makes it an interesting and promising tool to be utilised in industrial applications. Through enzyme immobilisation, biomolecules are confined onto/within a support or among the enzyme molecules itself thus enhancing structural rigidity and stability. This prevents dissociation of the enzyme subunits that could lead to enzyme inactivation, enables the enzyme to retain most of its catalytic activity and efficiency and leads to improved properties of the enzymes [8]. This technique can be categorised either as immobilisation with carrier or without carrier.

In recent years, a support-free immobilisation technique, *i.e.*, cross-linked enzyme aggregates immobilisation (CLEAs) has become more prevalent as it offers high productivities and enzyme recoveries by allowing separation from the products which in turns facilitates downstream processing by continuous operation. The cross-linking method

\* Corresponding author.

E-mail address: [r-rosli@utm.my](mailto:r-rosli@utm.my) (R.M. Illias).

<https://doi.org/10.1016/j.ijbiomac.2022.05.169>

Received 11 October 2021; Received in revised form 14 May 2022; Accepted 24 May 2022

Available online 27 May 2022

0141-8130/© 2022 Elsevier B.V. All rights reserved.

combines two processes; aggregation and immobilisation into one single operation to produce an immobilised enzyme with improved properties than that of free enzymes [3,9]. This involves physical precipitation of enzymes using a precipitant and followed by covalent interaction of one enzyme molecule to other enzyme molecules through suitable cross-linkers such as glutaraldehyde [10], chitosan [11] and dialdehyde starch [12]. In enzyme immobilisation, the cross-linking interactions between enzyme molecules and cross-linker have been validated to be the most stable. Nonetheless, the crosslinker needs to be a multifunctional agent to ensure that the biomolecules interact or cross-linked with each other in a network structure to establish strong covalent bonds [13,14].

Studies have been executed on many industrial enzymes such as lipase [15], laccase [16] and xylanase [17] using CLEAs technology. These studies reported that the catalytic performance and physical attributes of the immobilised enzymes were improved in comparison to free enzymes. Furthermore, they also demonstrated good reusability and storage stability for efficient utilisation of biocatalysts. The subtle modification of the cross-linking conditions provides an efficient solution to the drawbacks of free enzymes such as increased stability under harsh industrial reaction conditions, decreased substrate diffusional problems, recyclability as well as allowing tuning of enzyme selectivity and specificity [18,19]. This approach is highly economical as it is time- and cost-effective because no support material is needed, easy to scale-up and no requirement of highly purified enzyme [20].

Despite its advantages, this technology has not yet been fully utilised at industrial levels due to several gaps in fundamental information. Formation of stable and efficient CLEAs depends critically on the interaction of the amino acid residues with the cross-linker during the cross-linking process [21]. Low number of lysine on the enzyme's surface could affect the cross-linking formation and, in some cases, CLEAs will be extremely fragile after centrifugation [22]. However, the knowledge on protein orientation, type of amino acids and suitable location for the cross-linking process is very much lacking and unknown. These intermolecular interactions and formation of strong and stable enzyme aggregates are the major obstacles in CLEAs technology. These downsides must be addressed comprehensively in order to better understand the fundamentals of the carrier-free enzyme immobilisation approach to yield biocatalysts better suited for industrial applications.

Enzyme modification through site-directed mutagenesis by rational design is one of the oldest strategies that allows for the control of point attachment on the enzyme surface and the orientation of enzymes. Recent studies have exhibited that protein engineering is able to narrow down the orientation and coordination of amino acids whilst maintaining protein structure and conformation [23–25]. However, manipulation and changes of the structure and aggregation of enzyme molecules can affect the activity and stability of the enzyme.

Computer-aided molecular design is able to accurately forecast the conformational stability of protein structures as well as the reaction mechanisms and has contributed greatly to various research fields [26,27]. A combination of molecular dynamics simulation and structure analysis has enabled researchers to explain the increases in enzymatic activity by understanding the role of structural flexibility of the active site in enhancing the substrate accessibility [28] and the relationship between protein folding and various diseases [29]. The impacts of amino acids modification on enzyme stability, activity and binding with ligands can also be predicted using computational tools. This is of great importance as the attachment of cross-linkers to the enzyme surface in CLEAs has to be distant from the active site region to avoid any interference during the catalytic reaction [30].

Hence, a combined computational and experimental study was performed to understand and investigate the interaction of enzyme-CLEAs. In this study, maltogenic amylase from *Bacillus lehensis* G1 (Mag1) was chosen as the model enzyme based on our previous work [11]. Maltogenic amylases (EC 3.2.1.133) belong to glycoside hydrolase 13 (GH13) family together with  $\alpha$ -amylases (E.C 3.2.1.1), amylosucrases (EC

2.4.1.4) and dextran glucosidases (EC 3.2.1.70) among others. This group of enzymes catalyse the cleavage of  $\alpha$ -glycosidic linkages on substrates such as starch and cyclodextrins. They have wide applications in industries including pharmaceuticals, textiles and especially food industry [31,32]. Nevertheless, maltogenic amylases differ from other members of GH13 as its structure and architecture consist of an extra N-terminal domain that is recognised as carbohydrate binding module 34 (CBM34). This feature has led to the formation of a narrow and deep catalytic cavity [33,34].

Mag1-CLEAs has been developed using 80% concentrated ammonium sulfate (precipitating agent) and 0.25% (w/v) chitosan (cross-linker) [11]. The developed CLEAs has 58.1% activity recovery, and can be reused for up to 4 cycles whilst maintaining 20% activity. Nonetheless, the intermolecular interactions between the cross-linker and Mag1 were still not well explained. Therefore, this study was undertaken to clarify the interactions, to understand why certain amino acids at specific regions of the targeted enzymes are important in CLEAs formation and how this affects the stability, reusability and function of the enzymes. Surface modification of maltogenic amylase based on the molecular docking between Mag1 and crosslinker is expected to increase the cross-linking efficiency thus improving the performance and attributes of the biocatalyst.

## 2. Materials and method

### 2.1. Reagents and bacterial source

Restriction enzymes (*Xho*I and BamHI), Gibson Assembly® Cloning Kit, Q5® High-Fidelity 2× Master Mix and Monarch® DNA Gel Extraction Kit were purchased from New England Biolabs (Massachusetts, USA). Primers for protein engineering were synthesised by Integrated DNA Technologies, Iowa, USA. Affinity chromatography Ni-NTA agarose column (5 mL HisTrap HP) was purchased from Cytiva Life Sciences (Massachusetts, USA). Recombinant MAG1 from *Bacillus lehensis* G1 (GenBank accession number: KJ416416), pET21a(+) from Novagen (Darmstadt, Germany) and *Escherichia coli* BL21 (DE3) from Promega (Massachusetts, USA) were used throughout the study. Imidazole, isopropyl- $\beta$ -D-thiogalactoside (IPTG), DNA and protein markers, reagents and solvents used in this were of analytical grade or higher and are commercially available from Sigma Aldrich (Missouri, USA), Merck (Darmstadt, Germany), and Thermo Fisher Scientific (Massachusetts, USA).

### 2.2. In silico analysis

#### 2.2.1. Construction of Mag1 model structure and computational design of variants

Mag1 structure was built using MODELLER v9.23 [35] based on Abdul Manas (2016) [36] using the structure of neopullulanase (PDB ID: 1J0H) from *Bacillus stearothermophilus* TRS40 as the template. The constructed Mag1 structure and its amino acids were analysed using online tools; NetSurfP (<https://services.healthtech.dtu.dk/service.php?NetSurfP-2.0>), ResQ (<https://zhanglab.cmb.med.umich.edu/ResQ/>) and SPIDER3 (<https://sparks-lab.org/server/spider3/>) to determine the solvent-exposed amino acids. The distance between the exposed amino acids and catalytic region was measured using PyMOL and residues with the largest gap were chosen for modification. Furthermore, in order to determine the preferable orientation of CLEAs, amino acids on different secondary structure ( $\alpha$ -helix,  $\beta$ -sheet, coil) were also selected to be substituted. All graphical presentations of the models were prepared using PyMOL.

#### 2.2.2. Molecular docking and molecular dynamics simulation

The structure of Mag1 was docked with chitosan, glutaraldehyde, polylysine, glucosamine and ethylene glycol using Autodock Vina [37]. All cross-linker structures were obtained from PubChem [38]. After a

**Table 1**

List of primers used to construct Mag1 variants.

Fragment	Forward primer (5' – 3')	Reverse primer (5' – 3')
Mag1 (wild type)	CGCGGATCCATGAATCGAGCTGG	GGTGCTCGAGTGTGTGCGC
Mag1-mKc	GAAGCAAAGAAGAAGAAGATGCTTGCT	AGCAAGCATCTTCTTCTTCTTTGCTTC
Mag1-mKs	GCAACACAAACAGAAAAGAAGAAGAAACCG	CGGTTTTCTTCTTCTTCTTTCTGTTTGTGTTGC
Mag1-mKh	GCGTTATTAAGAAGAAGAAGAAGCAACTAGG	CCTAGTTGCTTCTTCTTCTTCTTCTTAATAACGC
Mag1-mKr	CCTAAGAAGAAGAAGGAGAAGTGGATGAAGCTTTTAC	GTAAGAAGCTTCATCCACTTCTCCTTCTTCTTAGG
Mag1-mDc	GAAGCAAAGGATGATGACGACATGCTTGCT	AGCAAGCATGTCGTCATCATCCTTTGCTTC
Mag1-mDs	GCAACACAAACAGAAAGCAAGGACGACAAACCG	CGGTTTTGTCGTCCTTGTCTTCTTTGTGTTGC
Mag1-mDh	GCGTTATTGATGATGACGACGATGACGATCAACTAGG	CCTAGTTGATCGTCGTCGTCATCATCAATAACGC
Mag1-mDr	CCTAAGGATGATGATGAGGACTGGATGGACCTTTTAC	GTAAGAAGTCCATCCAGTCTCATCATCCTTAGG

Underlined nucleotides: GGATCC: BamHI site. CTCGAG: XhoI site.**Bold nucleotides**: modified nucleotides.

thorough docking analysis, amino acids with the furthest distance from the active site (random) as well as on different secondary structures were substituted to lysine or aspartic acid. Structure for all variants were constructed, validated using SAVES 6.0 (<https://saves.mbi.ucla.edu/>) and subjected to blind molecular docking to determine the preferential amino acids by the cross-linker. The designated variants were as follows: Asp (D) substitution – Mag1-mDc (coil), Mag1-mDh ( $\alpha$ -helix), Mag1-mDs ( $\beta$ -sheet) and Mag1-mDr (random), and Lys (K) substitution – Mag1-mKc (coil), Mag1-mKh ( $\alpha$ -helix), Mag1-mKs ( $\beta$ -sheet) and Mag1-mKr (random). Results from the docking analysis were used to perform protein-ligand complex molecular dynamics simulation.

Protein topology of Mag1 and its variants were prepared using united atom GROMOS96 forcefield whilst ligand topology was prepared using ATB server (<https://atb.uq.edu.au/>) for molecular dynamics simulation. The coordinates of both protein and ligand topologies were combined to create a protein-ligand complex topology file. Simulation was performed using GROMACS4.6 [39] at 343 K with periodic boundary conditions, particle mesh Ewald summation and minimised to a steepest descent energy minimisation of 1000 steps. The structure was solvated with 1.0 nm simple point charge (SPC) water embedded in the simulation box. Then, sodium ions were added to replace water molecules and neutralise the system. The system was equilibrated for 50 ps of solute position-restrained. Root mean square deviations (RMSD), root mean square fluctuations, radius of gyration, hydrogen bonds and hydrophobic interactions were determined over 1000 ps production simulation for all backbone residues. Analyses of the molecular dynamics simulation were carried out using GROMACS utilities.

### 2.3. Development of Mag1 variants through site directed mutagenesis

Based on the computational analysis, a total of eight variants were generated by site directed mutagenesis approach. Primer sequences for each variant are listed in Table 1. Amplification was performed using polymerase chain reaction (PCR) reaction containing 10 ng DNA template, 1.5  $\mu$ M primer pair and 10  $\mu$ L KAPA Taq ReadyMix (2 $\times$ ) in a final volume of 20  $\mu$ L. The reaction was initiated with a pre-heating step of 5 min at 95  $^{\circ}$ C and 30 cycles of denaturation, annealing and extension phases of 95  $^{\circ}$ C for 30 s, 65  $^{\circ}$ C for 45 s and 72  $^{\circ}$ C for 5 min, respectively. The reaction was finalised with 10 min of final extension at 72  $^{\circ}$ C. The expression plasmid, pET21(+)*a* was digested with BamHI and XhoI for 10 min and the linearised plasmid and gene fragment for each variant were assembled using the Gibson Assembly method [40].

*E. coli* BL21 cells were transformed with plasmids carrying the modified MAG1 gene, plated onto Luria-Bertani agar containing 100  $\mu$ g/mL ampicillin and incubated overnight at 37  $^{\circ}$ C. Then, random colonies were picked and screened with PCR and restriction enzymes digestions to ensure amplification reactions did not led to wrong plasmid constructions due to strand displacement during the elongation step. The products were validated by agarose gel electrophoresis and mutations were verified by DNA sequencing.

### 2.4. CLEAs preparation and enzymatic assay

Mag1 and Mag1 mutants were produced as per previous report [41] and the development of Mag1-CLEAs and CLEAs of Mag1 variants (henceforth referred to as variant-CLEAs) were as aforementioned in Nawawi et al. (2020) [11]. Briefly, 150 U (approximately 5 mg) of purified enzyme in 50 mM potassium phosphate buffer pH 7.0 was added to precipitating agent (80% saturated ammonium sulfate) and aggregated by incubation at 4  $^{\circ}$ C for 1 h with continuous shaking (150 rpm). Then, the mixture was added with 0.25% (w/v) chitosan or 0.25% (v/v) glutaraldehyde and the incubation allowed to proceed for another 1.5 h to complete the cross-linking process. The developed CLEAs particles were centrifuged for 10 min at 11, 337  $\times$ g to remove salt, crosslinkers and remaining free enzymes that were not cross-linked. Next, the particles were washed two times using potassium phosphate buffer (50 mM, pH 7.0) and resuspended in the same buffer for further analysis. The enzymatic assay and recovery activity calculation of both soluble and immobilised enzymes were performed as previously reported [7]. The enzymatic assay and activity recovery calculation of both soluble and immobilised enzymes were performed as reported [11] as below:

$$\text{Enzyme activity} \left( \frac{U}{mL} \right) = \frac{\text{reducing sugar} (\mu\text{mol}) \times \text{total assay volume} (mL)}{\text{enzyme volume} (mL) \times \text{time of assay} (min)} \quad (1)$$

$$\text{Activity recovery} (\%) = \frac{\text{Total Mag1 activity in Mag1-CLEAs} (U)}{\text{Total Mag1 activity used for CLEAs preparation} (U)} \times 100 \quad (2)$$

### 2.5. Biophysical characterisation

Biophysical characterisation of Mag1-CLEAs and variant-CLEAs were performed as previously reported by Nawawi et al. (2020) [11]. The surface morphology of Mag1- and variant-CLEAs were examined under a field emission scanning electron microscope (FESEM) (Hitachi SU8020, USA). The functional groups of Mag1- and variant-CLEAs were analysed using Fourier Transform Infrared (FTIR) spectroscopy (Perkin Elmer, Ohio, USA) in the wavenumber range of 370–4000  $\text{cm}^{-1}$ . Prior to FESEM and FTIR, the samples were vacuum concentrated to remove excess water using Eppendorf Concentrator Plus™ (Eppendorf AG, Hamburg, Germany). Particles size analysis of the CLEAs was measured using Malvern Zetasizer Nano ZSP (Malvern Panalytical, Malvern, UK).

### 2.6. Stability and enzyme kinetics characterisation

Biochemical characterisation of Mag1- and variant-CLEA was performed as previously described by Nawawi et al. (2020) [11]. The effect of pH was determined by preincubating the CLEAs in buffers of different pH (pH 4.0–10.0) at 4  $^{\circ}$ C for 1 h without substrate. After incubation, the remaining activity was measured by the standard assay [30]. For

**Table 2**  
Binding energy of Mag1 and its variants with different cross-linkers in docking analysis.

Variants	Chitosan (kcal/mol)	Ethylene glycol (kcal/mol)	Polylysine (kcal/mol)	Glucosamine (kcal/mol)	Glutaraldehyde (kcal/mol)
Mag1	-7.5	-5.1	-5.0	-5.8	-3.4
Mag1-mKc	-6.4	-5.5	-4.2	-3.1	-4.9
Mag1-mKs	-7.2	-4.0	-4.7	-4.1	-4.7
Mag1-mKh	-6.6	-5.4	-4.8	-3.0	-5.1
Mag1-mKr	-7.2	-5.4	-4.4	-4.2	-4.4
Mag1-mDc	-8.0	-5.1	-5.3	-5.4	-4.0
Mag1-mDs	-8.5	-5.7	-5.8	-4.6	-4.6
Mag1-mDh	-8.5	-5.2	-6.1	-5.2	-4.6
Mag1-mDr	-7.8	-4.3	-5.5	-6.0	-3.8

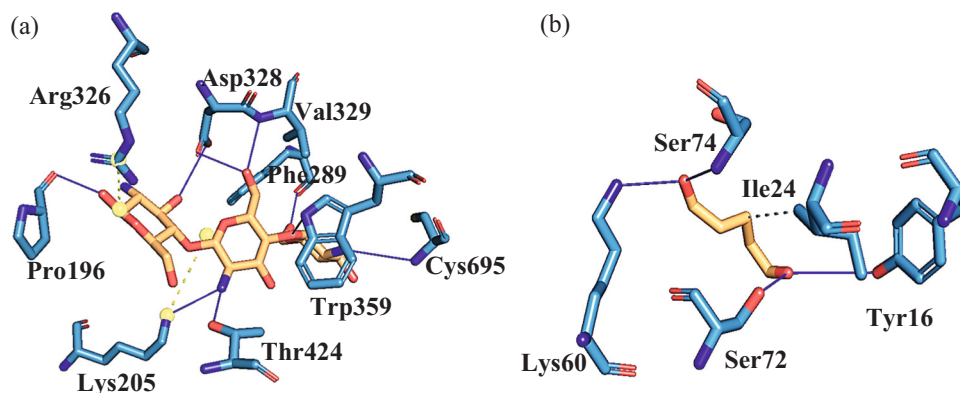


**Fig. 1.** Docking analysis between of Mag1 and crosslinkers. (a) Mag1-chitosan; (b) Mag1-glutaraldehyde. Blue line represents covalent interaction, yellow dashed line represents disulfide bridge and grey dashed line represents hydrophobic interaction. (For interpretation of the references to colour in this figure legend, the reader is referred to the web version of this article.)

determination of thermostability, the CLEAs were pre-incubated in 50 mM phosphate buffer pH 7.4 at different temperatures (30–80 °C) for 1 h. Then, the standard assay protocol was performed to determine residual activity of the CLEAs. The residual activity for stability analysis was calculated and the initial activity was defined as 100%. The experiment was performed in triplicate to ensure data reproducibility.

The apparent kinetic parameters of the developed CLEAs were investigated using various  $\beta$ -CD concentrations under the optimal conditions. Specific activity (U/mg), maximum velocity ( $V_{max}$ ), Michaelis-Menten constant ( $K_m$ ), turnover number ( $k_{cat}$ ) and catalytic efficiency ( $k_{cat}/K_m$ ) were determined from the Lineweaver Burk plot.

## 2.7. Reusability analysis

The recyclability attribute of Mag1- and variant-CLEAs were assessed by performing DNA assay repeatedly [11] for 8 cycles. After each cycle, the immobilised enzymes were recovered by centrifugation (3 min, 14,000  $\times$ g) followed by washing three times with 50 mM potassium phosphate buffer pH 7.0 and resuspended in fresh reaction mixture. The activity of Mag1- and variant-CLEAs was measured under standard assay conditions. Enzyme activity from the first cycle was set as 100% and the residual activity of the immobilised enzyme was calculated after each successive cycle.

## 3. Results and discussion

### 3.1. Construction of Mag1 variants

The amino acid sequence and structure of Mag1 were subjected to computational analyses to determine suitable modification sites for covalent cross-linking interactions. Based on the docking simulation, it was shown that Mag1 has the lowest binding energy towards chitosan (-7.1 kcal/mol), followed by glucosamine (-5.8 kcal/mol) and

ethylene glycol (-5.0 kcal/mol) whilst interaction with glutaraldehyde yielded the highest energy (-3.6 kcal/mol) (Table 2). A lower binding energy in a ligand-bound complex was presumed to resemble the native state and is more stable compared to a higher binding energy complex [42]. This analysis is also in agreement with the study that reported chitosan as the best cross-linker for Mag1 whereas other cross-linkers yielded low recovery activity [11]. Therefore, subsequent investigation was focused on chitosan and glutaraldehyde as it is the optimal cross-linker for Mag1 and universal cross-linker for CLEAs [3], respectively.

Further analysis on all docking conformations revealed that chitosan and glutaraldehyde have a preference towards aspartic acid (Asp) and lysine (Lys), respectively (Fig. 1 and Supplementary 1). Analysis on different docking conformations revealed that Lys was preferred by glutaraldehyde (23%) whilst Asp was preferred by chitosan (44%). Based on the docked structures, it was observed that chitosan established interactions associated with Lys205, Phe289, Arg326, Asp328, Val329, Trp359, Thr424 and Cys695 whilst glutaraldehyde interacts with Ile 24, Tyr16, Lys60, Ser72 and Ser74. Covalent coupling requires the presence of reactive functional groups on the surface of proteins and ligands. According to Redeker et al. (2013) [43], amines (-NH<sub>2</sub>) and carboxylic acids (-COOH) groups are the most commonly used moieties for covalent immobilisation which could explain the preference of amino acids by glutaraldehyde and chitosan. Surface area of Mag1 revealed that out of 580 amino acids, 166 residues were exposed on the surface with 14 and 20 of them being lysine and aspartic acid residues, respectively. Therefore, it was proposed that by increasing the number of lysine and aspartic acid residues on the Mag1 surface, the crosslinking efficiency and covalent binding with glutaraldehyde and chitosan will be improved accordingly.

Determination of the substitution sites is crucial to ensure that the cross-linking does not interfere with substrate diffusion into the active site as well as maintaining the structure architecture. In addition, the

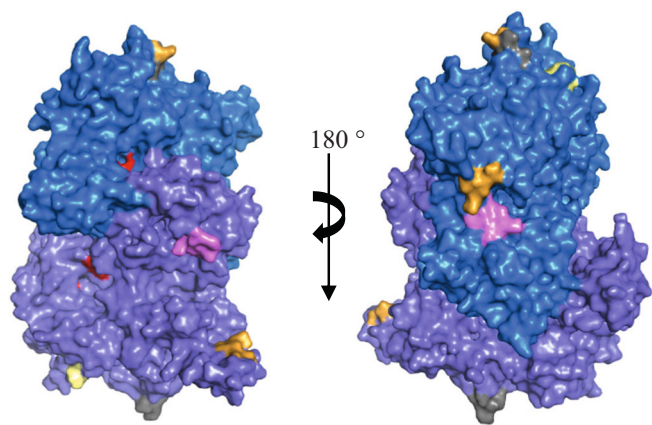


**Fig. 2.** Surface modification sites of Mag1 variants. Catalytic site is displayed in red, random mutation sites in orange, coil site in grey,  $\alpha$ -helix in yellow and  $\beta$ -sheets in pink. (For interpretation of the references to colour in this figure legend, the reader is referred to the web version of this article.)

**Table 3**  
Enzymatic activity of Mag1 and Mag1 variants.

	Enzyme activity (U/mL)	Total activity (U)	Total protein (mg)	Specific activity (U/mg)
MAG1	1637.9 $\pm$ 0.4	4913.6 $\pm$ 0.9	30.5 $\pm$ 0.3	161.1 $\pm$ 1.1
Mag1-mKc	1463.8 $\pm$ 3.1	4391.5 $\pm$ 2.3	27.9 $\pm$ 0.8	157.4 $\pm$ 0.4
Mag1-mKs	1747.7 $\pm$ 0.3	5243.2 $\pm$ 3.1	31.7 $\pm$ 0.4	165.4 $\pm$ 0.6
Mag1-mKh	1688 $\pm$ 0.7	5064.1 $\pm$ 0.5	32.4 $\pm$ 2.2	156.3 $\pm$ 3.9
Mag1-mKr	1484 $\pm$ 0.2	4452 $\pm$ 0.9	26.9 $\pm$ 0.3	165.5 $\pm$ 0.7
Mag1-mDc	1854.5 $\pm$ 0.4	5563.4 $\pm$ 0.2	32.9 $\pm$ 0.6	169.1 $\pm$ 0.2
Mag1-mDs	1705.8 $\pm$ 0.8	5117.3 $\pm$ 1.5	33.6 $\pm$ 0.5	152.3 $\pm$ 1.6
Mag1-mDh	1621.6 $\pm$ 0.2	4864.8 $\pm$ 0.6	28.3 $\pm$ 2.9	171.9 $\pm$ 0.4
Mag1-mDr	1510.1 $\pm$ 0.7	4530.2 $\pm$ 0.3	35.2 $\pm$ 3.4	128.7 $\pm$ 0.8

**Table 4**  
Recovery activity of Mag1 variants cross-linked with glutaraldehyde or chitosan.

	Recovery activity CLEA-glutaraldehyde (%)	Recovery activity CLEA-chitosan (%)
MAG1	44.3 $\pm$ 3.1	63.5 $\pm$ 2.4
Mag1-mKc	49.3 $\pm$ 4.2	65.7 $\pm$ 3.9
Mag1-mKs	53.7 $\pm$ 3.3	67.4 $\pm$ 1.5
Mag1-mKh	54.5 $\pm$ 2.6	67.1 $\pm$ 2.7
Mag1-mKr	47.6 $\pm$ 1.7	63.9 $\pm$ 3.2
Mag1-mDc	42.9 $\pm$ 2.9	75.5 $\pm$ 4.3
Mag1-mDs	44.6 $\pm$ 2.1	80.7 $\pm$ 3.7
Mag1-mDh	46.1 $\pm$ 3.3	83.2 $\pm$ 2.9
Mag1-mDr	43.2 $\pm$ 5.3	78.3 $\pm$ 4.1

selected amino acids must not lead to enzyme inactivation or instability [44]. Thus, based on the distance of the exposed amino acid and the catalytic region, five amino acids (E548, Q552, Q550, N549, D482) were

chosen to be mutated to either Lys or Asp as they fit the aforementioned criteria. Other than amino acid preferences, cross-linking orientation is also another factor that is important as interfacial cross-linking orientation could improve functions, enhance stability and increase shelf-life of biocatalysts [45]. By possessing long shelf-life stability, immobilised biocatalysts are able to tolerate long-term storage without significant loss in catalytic activity and stereoselectivity [46]. For this purpose, different secondary structures ( $\alpha$ -helix,  $\beta$ -sheet or coil) that are the furthest from the active site were also selected to be substituted. Hence, Lys or Asp was introduced at amino acid Q180, H181, D183, Y184, Q186 for mutation at  $\alpha$ -helix, M59, L60, L62 for  $\beta$ -sheet, and Q481, D482, D484 for coil structure (Fig. 2). Thus, in total, eight variants of Mag1 (Mag1-mDc, Mag1-mDh, Mag1-mDs, Mag1-mDr, Mag1-mKc, Mag1-mKh, Mag1-mKs and Mag1-mKr) were designed and constructed depending on the amino acid substitution and selected secondary structure region for further analysis. The amino acids modification on each variant are listed in Supplementary 2.

Structure models for all variants were built and validated to verify that no conformational changes occurred due to the amino acid substitution (Supplementary 2). The results indicated that the backbone dihedral angle for all variants was of satisfactory quality and credible to be used for further investigations. Besides, no buried amino acids were replaced to a maintained interior conformation of Mag1 variants. Mutant structures were also docked with cross-linkers and it showed better scoring in binding energy than that of Mag1 wild type (Table 2). Among all variants, Mag1 mutated with Asp at  $\alpha$ -helix (Mag1-mDh) and  $\beta$ -sheets (Mag1-mDs) displayed the lowest binding affinity ( $-8.5$  kcal/mol) when cross-linked with chitosan. Variants with Lys substitution also showed an increase in binding energy when cross-linked with glutaraldehyde with Mag1-mKh (substitution at  $\alpha$ -helix) displaying the lowest binding energy ( $-5.1$  kcal/mol). These results verify that the selected sites for mutagenesis were reliable and could be proceeded for subsequent investigation.

### 3.2. Enzymatic activity of soluble and immobilised enzymes

Mag1 and Mag1 variants were recombinantly expressed, purified and their enzymatic activities were determined under standard conditions (Table 3). It was shown that the activity of Mag1 was 161.1 U/mg whereas the maximum activity of mutants (171.9 U/mg) is from Mag1-mDh. All variants exhibited similar enzymatic activity as Mag1 thus corroborating the *in-silico* analysis that the selected sites for amino acids substitution did not affect the catalytic site conformation or the activity. As protein engineering can lead to chemical changes around the enzyme catalytic site [47] hence, it is crucial that the intermolecular interactions between the enzyme molecules and cross-linker is formed outside or far from the catalytic region in order to control enzyme kinetics and performance [48].

CLEAs for Mag1 and its variants were developed and the activity recovery for all immobilised enzymes was measured (Table 4). It was shown that when the variants were cross-linked with chitosan, those with Asp modification (Mag1-mDc, Mag1-mDs, Mag1-mDh and Mag1-mDr) exhibited notable increment in the activity recovery compared to the Mag1-CLEAs (63.5%). Mag1-mDh-CLEAs displayed the highest recovery (83.2%) and this is followed by Mag1-mDs-CLEAs (80.7%). In addition, variants with Lys modification (Mag1-mKc, Mag1-mKs, Mag1-mKc and Mag1-mKr) were revealed to have preferences towards glutaraldehyde as cross-linker with Mag1-mKh-CLEAs exhibiting the highest recovery of 54.5% than Mag1-CLEAs (44.3%). The aldehyde groups of glutaraldehyde have been proven to favour interaction with the  $\epsilon$ -amino group of lysine to form stable imine linkages [49,50].

CLEAs with modification on  $\alpha$ -helix and  $\beta$ -sheets structures were shown to have higher recovery activity than CLEAs modified on coil or random sites. Controlling protein orientation is crucial to ensure optimal functionality of immobilised proteins [43]. Thus, oriented immobilisation could be the reason of an increase in activity recovery for variant-

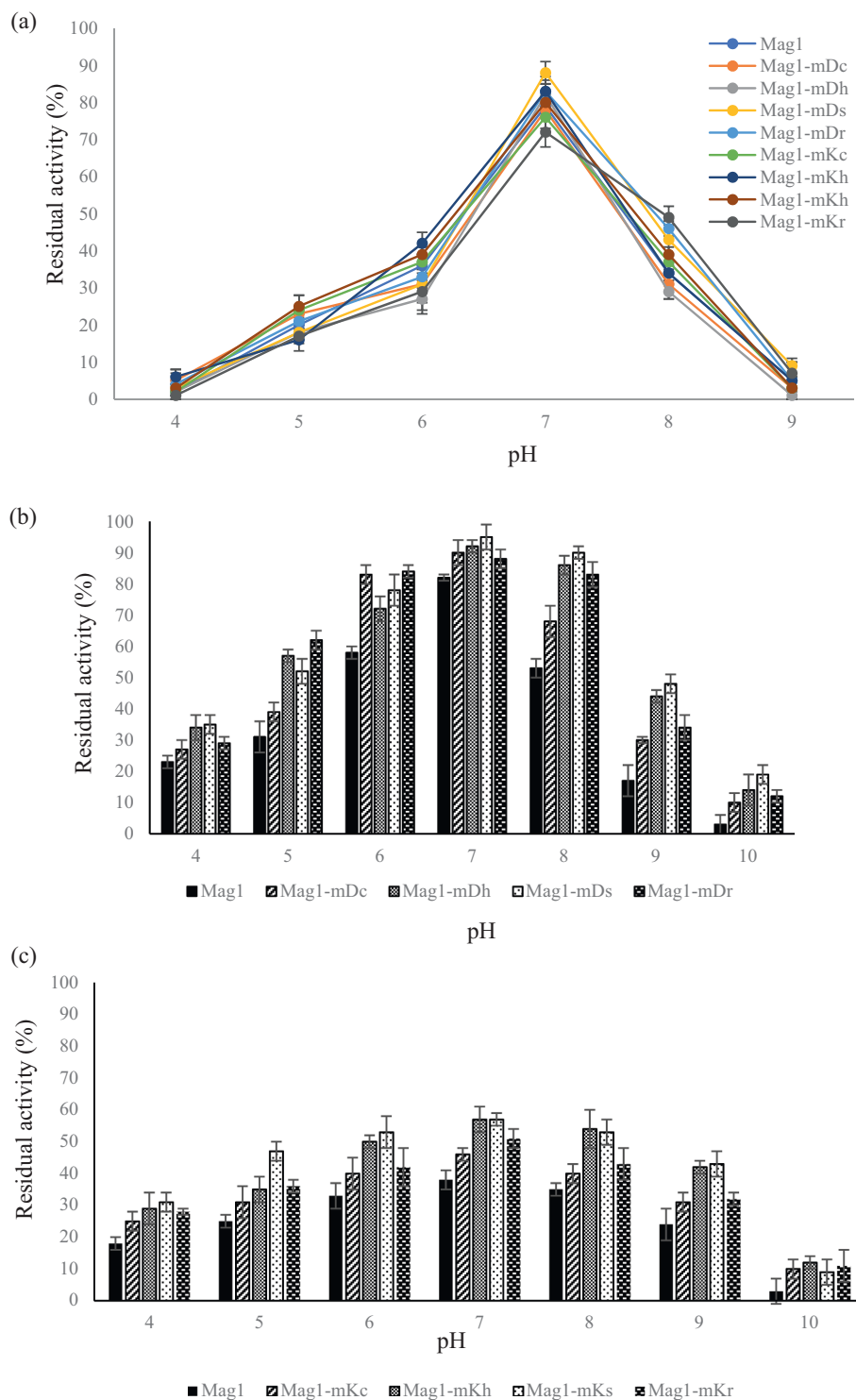
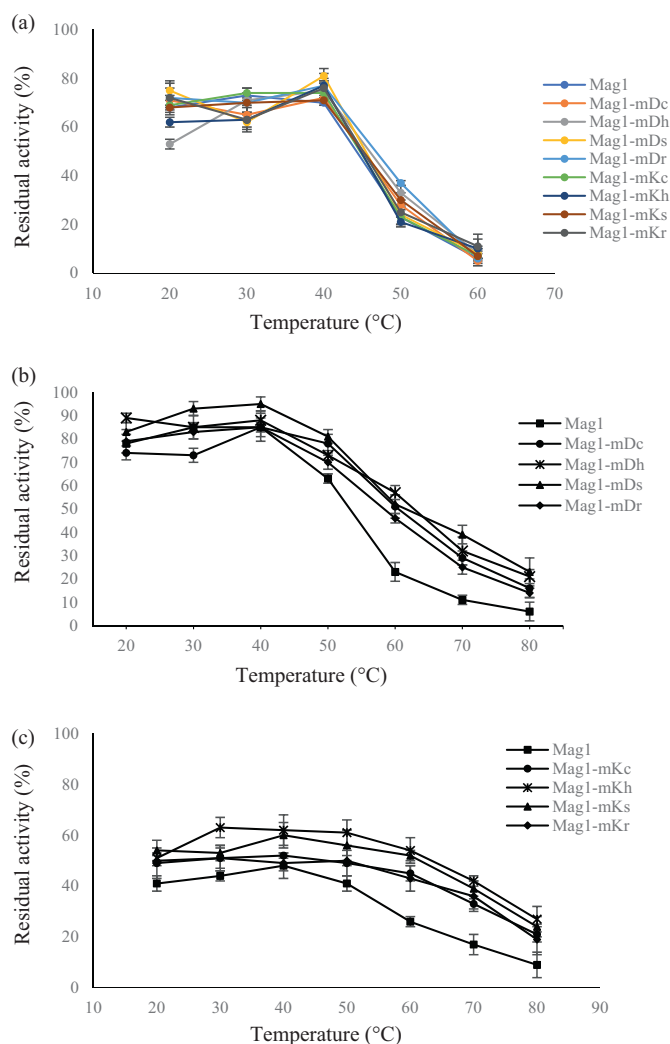


Fig. 3. pH stability profile of soluble enzymes and CLEAs. (a) Free enzyme, (b) CLEAs cross-linked with chitosan, and (c) CLEAs cross-linked with glutaraldehyde. All experiments were conducted in triplicate and the error bar represents the standard deviation.

CLEAs as it provides optimal accessibility of substrate towards active site that is tunable in the direction of the environment. The linear structures and abundant presence of reactive amine and hydroxyl groups in chitosan [51] and dialdehyde groups in glutaraldehyde [52] might promote efficient intermolecular interactions between both cross-linker and Mag1 variants, hence improving the enzymatic activity. However, no notable differences were observed in the activity recovery of Lys-modified variant-CLEAs cross-linked with chitosan or Asp-modified

variant-CLEAs cross-linked with glutaraldehyde when compared with Mag1-CLEA-chitosan or Mag1-CLEA-glutaraldehyde, respectively. Thus, this shows that the cross-linkers have preferences towards specific amino acids. Based on these results, further investigations were only carried out on the following combinations: Lys-modified variant-CLEAs cross-linked with glutaraldehyde and Asp-modified variant-CLEAs cross-linked with chitosan.



**Fig. 4.** Thermal stability profile of Mag1 and its derivatives. (a) Soluble enzymes; (b) CLEAs cross-linked with chitosan; (c) CLEAs cross-linked with glutaraldehyde. All experiments were conducted in triplicate and the error bars represent the standard deviation.

### 3.3. Stability and reusability characterisations of CLEAs

The stability performances of both free enzymes and developed CLEAs were investigated in different pHs (pH 3–10) and temperatures (20–80 °C). As illustrated in Fig. 3a, all free enzymes have similar pattern of pH stability after incubation in buffers of different pHs for 1 h. Although they were most stable at pH 7.0 but other pHs affected the stability of the enzymes significantly. Notably, the developed CLEAs were less affected by pH acidity and alkalinity than their soluble counterparts (Fig. 3b and c). It was exhibited that all variants -CLEAs have a higher stability compared to Mag1-CLEAs and still retained around 15% residual activity at pH 10, whereas Mag1-CLEAs lost about 96% activity after incubation in the same pH. It is also clear that CLEAs developed using glutaraldehyde (Lys substitution) have lower residual activity compared to those developed using chitosan (Asp substitution). However, this is expected as enzymes cross-linked with glutaraldehyde also yielded lower recovery activity compared to enzymes cross-linked with chitosan as discussed in Section 3.2.

The temperature profiles revealed that all soluble enzymes displayed similar stability trends and retain more than 50% residual activity for temperatures between 20 and 40 °C (Fig. 4a). Nonetheless, the stability for all free enzymes decreases rapidly after incubation at 50 °C (20 to

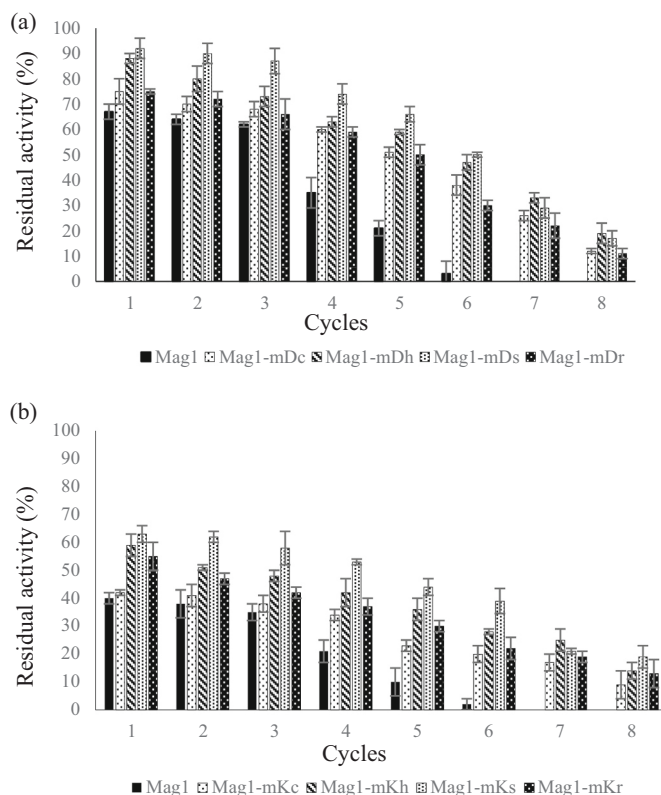


**Fig. 5.** Reusability of Mag1- and variant-CLEAs. (a) CLEAs of Mag1 and Asp substituted variants; (b) CLEAs of Mag1 and Lys substituted variants. All experiments were conducted in triplicate and the error bars represent the standard deviation.

**Table 5**

Apparent kinetics values of soluble and immobilised enzymes.

	$V_{max}$ ( $\mu\text{molml}^{-1}\text{min}^{-1}$ )	$K_m$ (mM)	$k_{cat}$ ( $\text{s}^{-1}$ )	$k_{cat}/K_m$ ( $\text{mM}^{-1}\text{s}^{-1}$ )
Mag1	6.17	3.94	6.73	2.29
Mag1-mDc	5.98	3.84	6.21	2.19
Mag1-mDh	6.57	3.39	6.77	1.99
Mag1-mDs	5.72	3.31	7.32	2.70
Mag1-mDr	6.41	4.13	6.95	2.22
Mag1-mKc	5.59	4.16	6.53	2.55
Mag1-mKs	6.23	3.62	7.46	2.06
Mag1-mKh	6.16	3.54	6.02	1.70
Mag1-mKr	5.81	3.59	7.34	2.04
CLEAs cross-linked with chitosan				
Mag1-CLEAs	4.24	2.91	4.21	1.45
Mag1-mDc	5.32	2.16	5.88	2.72
Mag1-mDh	5.94	1.58	5.36	3.39
Mag1-mDs	5.67	0.97	4.16	4.29
Mag1-mDr	6.03	2.22	5.72	2.57
CLEAs cross-linked with glutaraldehyde				
Mag1-CLEAs	3.43	3.29	3.65	1.11
Mag1-mKc	4.78	2.56	6.82	2.66
Mag1-mKh	5.92	1.83	5.18	2.83
Mag1-mKs	6.05	1.16	4.84	4.17
Mag1-mKr	5.51	2.24	6.35	2.83

35% residual activity) and lost almost all activity at 60 °C. In comparison, the immobilised enzymes displayed a higher resistance towards temperature changes (Fig. 4b and c) and all variant-CLEAs retained

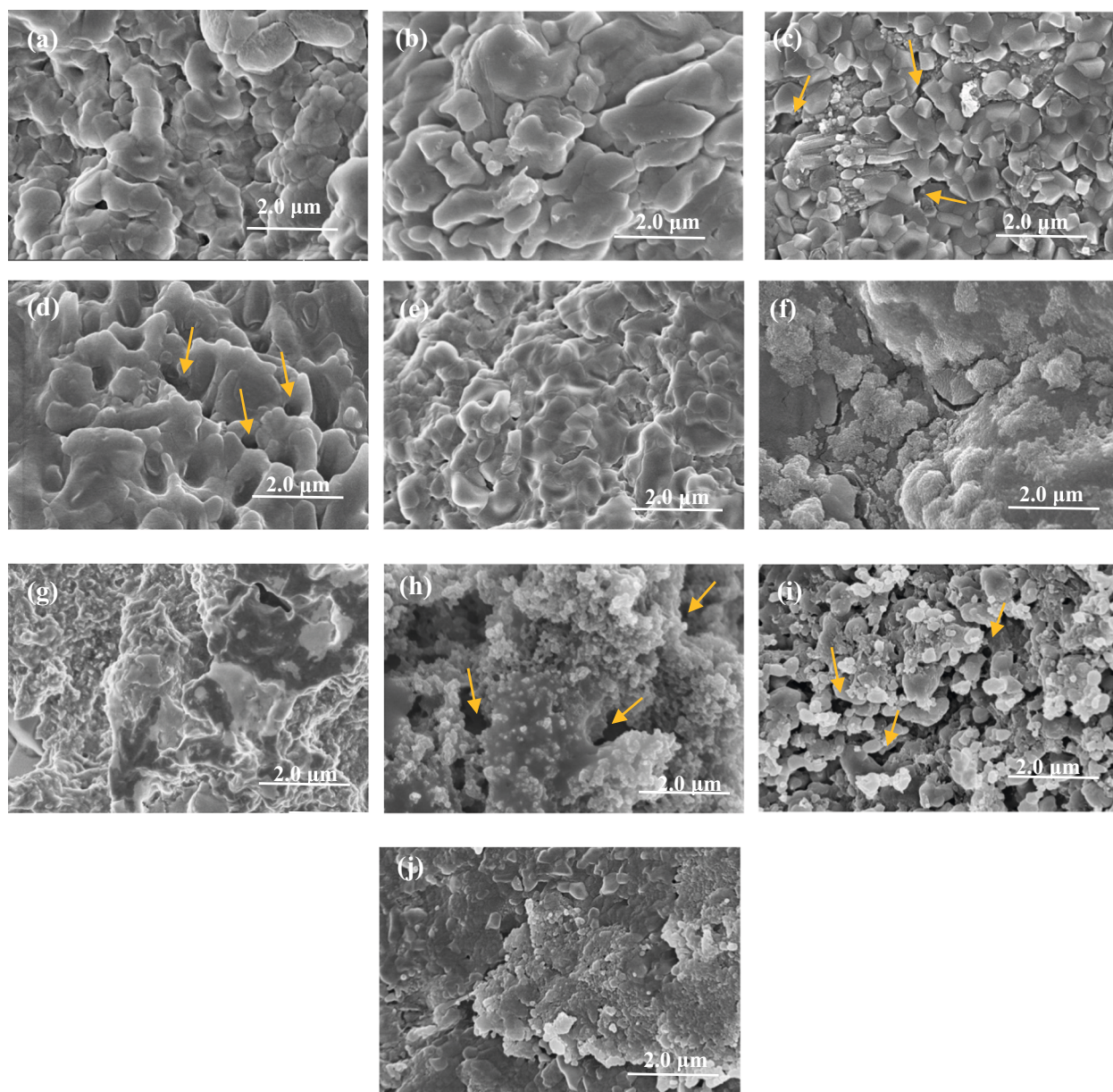


**Fig. 6.** FESEM images of Mag1- and variant-CLEAs. (a) Mag1-CLEAs cross-linked with chitosan; (b) Mag1-mDc-CLEAs; (c) Mag1-mDh-CLEAs; (d) Mag1-mDs-CLEAs; (e) Mag1-mDr-CLEAs; (f) Mag1-CLEAs cross-linked with glutaraldehyde (g) Mag1-mKc-CLEAs; (h) Mag1-mKh-CLEAs; (i) Mag1-mKs-CLEAs; (j) Mag1-mKr-CLEAs. Cavities on the CLEAs surface are indicated by orange arrows. The magnification used for all images was  $\times 20,000$ . (For interpretation of the references to colour in this figure legend, the reader is referred to the web version of this article.)

higher residual activity than that of Mag1-CLEAs. At 80 °C, Mag1-CLEAs activity was reduced to approximately 6–9%, whereas all variant-CLEAs still retained 20–30% of activity. Out of eight variants, Mag1-mDs-CLEAs and Mag1-mKh-CLEAs displayed the highest thermal stability. Interestingly, at elevated temperatures, Lys-modified variants exhibited a slower decrease in residual activity compared to Asp-modified variants. This occurrence could be due to the composition or chemistries of the cross-linker itself. Exposure to high temperatures (more than 40 °C) will cause significant loss of moisture or dehydration to chitosan thus decreasing its hardness and mechanical strength [53]. The N–H stretching region of chitosan was reported to decrease at high temperatures and is suggested to decrease the intermolecular interactions of chitosan [54]. As for glutaraldehyde, exposure to 40 °C for eight weeks only decreases 36% of its efficiency [55]. In addition, the group also pointed that degradation products of glutaraldehyde (dimer, oligomers) by temperature may increase protein cross-linking efficiency compared

to the monomer of glutaraldehyde.

One of the attractive attributes of an immobilised enzyme is their recyclability and easy enzyme recovery. The reusability trials were carried out for all immobilised enzymes in consecutive cycles to demonstrate their feasibility for industrial use. As illustrated in Fig. 5, all CLEAs still retained similar activity as the initial activity after three repeated cycles. However, Mag1-CLEAs lost almost half of the activity after cycle four and managed to retain about 2% of the initial activity in cycle six, whilst the variant -CLEAs still possessed about 20–50% activity for both chitosan and glutaraldehyde cross-linkers. After eight consecutive cycles, the remaining activities of variants cross-linked with chitosan and glutaraldehyde were between 9–19% and 11–20%, respectively. A reduction in activity with increasing number of reactions was presumably due to alteration in CLEAs morphology and enzyme leaching during repeated washing at the end of each cycle. In addition, the solution microenvironment might also cause alteration in the

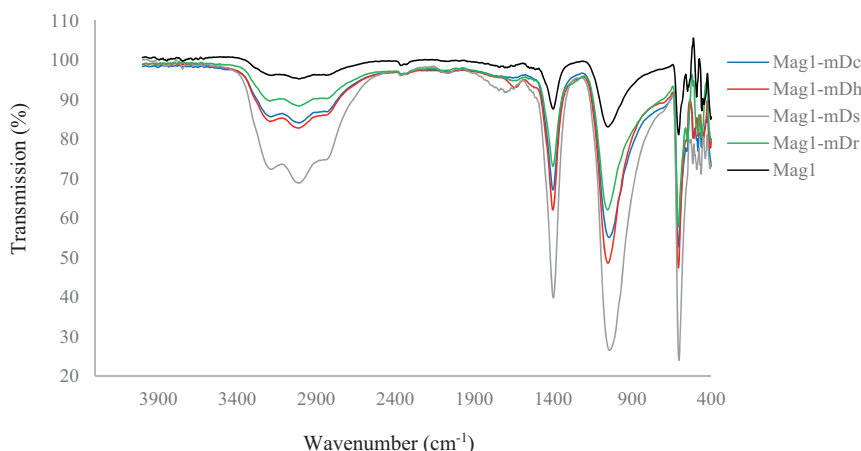


Fig. 7. Fourier Transform infrared (FTIR) profile of Mag1- and Asp-variant-CLEAs.

integrity of enzyme conformation during the recycling process and hence leading to the loss of enzyme activity [56].

The ability of immobilised enzymes to exhibit greater functional properties such as high stability and the ability to be used in continuous reaction cycles advocate their practicality and make them desirable candidates to be implemented at commercial scales. According to Parveen et al. (2021) [57], charge alterations in amino acids residues as well as slight modification on the structural conformation commonly occurs in the developed CLEAs. This is due to aggregation and cross-linking formation between enzyme and cross-linkers.

In this study, several surface amino acids were substituted to Lys or Asp to improve the tethering interactions between Mag1 and cross-linkers. Lysine with its amine functional group is very reactive towards electrophilic agents such as dialdehydes, whilst aspartic acid with its carboxylic side chain can easily form covalent interactions with amines [43,58,59]. Therefore, modification of amino acids to Lys or Asp is expected to enhance the intermolecular interactions due to the formation of new linkages between the amino acids and cross-linkers during CLEAs formation. These additional interactions reduce conformational elasticity of the enzyme thus protecting CLEAs from distortion or denaturation [60]. Furthermore, it also changes the microenvironment of the immobilised enzyme thus influencing the catalytic performance [61]. This may explain why variant-CLEAs are more stable, resistant to denaturation, and reusable compared to Mag1-CLEAs.

Interestingly, it was noticed that even though Asp-variant-CLEAs have a higher activity recovery than Lys-variant-CLEAs, they have a lower stability and their activity decreases more rapidly than the latter CLEAs. This could be due to the size of glutaraldehyde which is smaller than chitosan [59], thus generating CLEAs particles that are more compact and able to endure harsher surroundings. It was also observed that a more oriented immobilisation ( $\alpha$ -helix and  $\beta$ -sheet) yielded CLEAs with higher activity recovery and stability than random site-specific CLEAs (Mag1-mDr and Mag1-mKr). According to Zou et al. (2018) [62] and Li et al. (2018) [63], orientational flexibility may lead to an unfavourable orientation on the immobilised protein surface, thus affecting its activity and rigidity. Of all the oriented immobilisations, variant-CLEAs with amino acid substitution on  $\beta$ -sheet (Mag1-mDs and Mag1-mKs) were shown to have higher stability compared to other variants. It was reported that the mechanical force and steady-state of the  $\beta$ -sheet structure are superior to  $\alpha$ -helix and coil structures [64]. Hence, combining these properties with increased intermolecular interactions could justify Mag1-mDs and Mag1-mKs performances.

### 3.4. Kinetic analysis of CLEAs

The kinetic parameters ( $K_m$ ,  $V_{max}$ ,  $k_{cat}$  and  $k_{cat}/K_m$ ) for soluble enzymes and CLEAs were measured using Lineweaver Burk plot (Table 5).

As presented, all soluble enzymes displayed similar kinetic values indicating that the amino acid modification did not lead to any major changes around the active site region. This is important because CLEAs formation will reduce enzymatic activity as a trade-off for stability. Therefore, it is crucial to have variants with comparable catalytic ability as the wild-type.

From the kinetics analysis, it was shown that all CLEAs have a lower  $V_{max}$  than the free enzymes, especially Mag1-CLEAs indicating that the immobilised enzyme converted less substrate to product per unit of time upon saturation with substrates. This is probably due to the formation of compact aggregates that hinder substrate accessibility to the active site [15].

In addition, the apparent  $K_m$  for all immobilised enzymes was observed to have a lower value than their soluble counterparts. Variants substituted at the  $\beta$ -sheets region; Mag1-mDs (0.97 mM) and Mag1-mKs (1.16 mM) exhibited the highest affinity among all CLEAs, relative to their respective cross-linking agent. Enzyme interactions with its substrate are specified through  $K_m$  values [65,66] and these results indicate that after the aggregation and cross-linking processes, structural conformation changes are likely to occur that result in higher affinity towards the substrate. Proper complex formation [67] and suitable orientation [63] between the immobilised enzyme and substrate could be the reason of the improved interaction.

As shown in the table, all immobilised enzymes have a lower  $k_{cat}$  demonstrating that the catalysis rate of CLEAs is slower than the free enzymes. Despite that, all enzymes excluding Mag1, exhibited an increase in hydrolytic efficiency towards  $\beta$ -CD after being immobilised with chitosan or glutaraldehyde. As expected, immobilised variants with modification on a more structured conformation ( $\alpha$ -helix and  $\beta$ -sheets) fared better in terms of catalytic efficiency ( $k_{cat}/K_m$ ) than variants with modification on coil or random sites. It was also noted that, CLEAs with amino acids modification on  $\beta$ -sheets; Mag1-mKs ( $4.17 \text{ mM}^{-1} \text{ s}^{-1}$ ) and Mag1-mDs ( $4.29 \text{ mM}^{-1} \text{ s}^{-1}$ ) have the highest efficiency among all variants. This is attributed to the decrease of  $K_m$  value, thus confirming the idea that improved enzymatic properties and immobilisation orientation are crucial in the development of CLEAs. The enhanced performance could also possibly be due to the presence of cavities on the surface of the CLEAs particles [12] hence creating more areas for substrate accessibility.

### 3.5. CLEAs morphology and size

The morphology of the developed CLEAs was analysed using FESEM (Fig. 6). The aggregates of CLEAs cross-linked with chitosan have a larger spherical, more distinct and structured surface than CLEAs cross-linked with glutaraldehyde. This is probably due to the size and properties of the cross-linkers used to develop the CLEAs. Variant-CLEAs

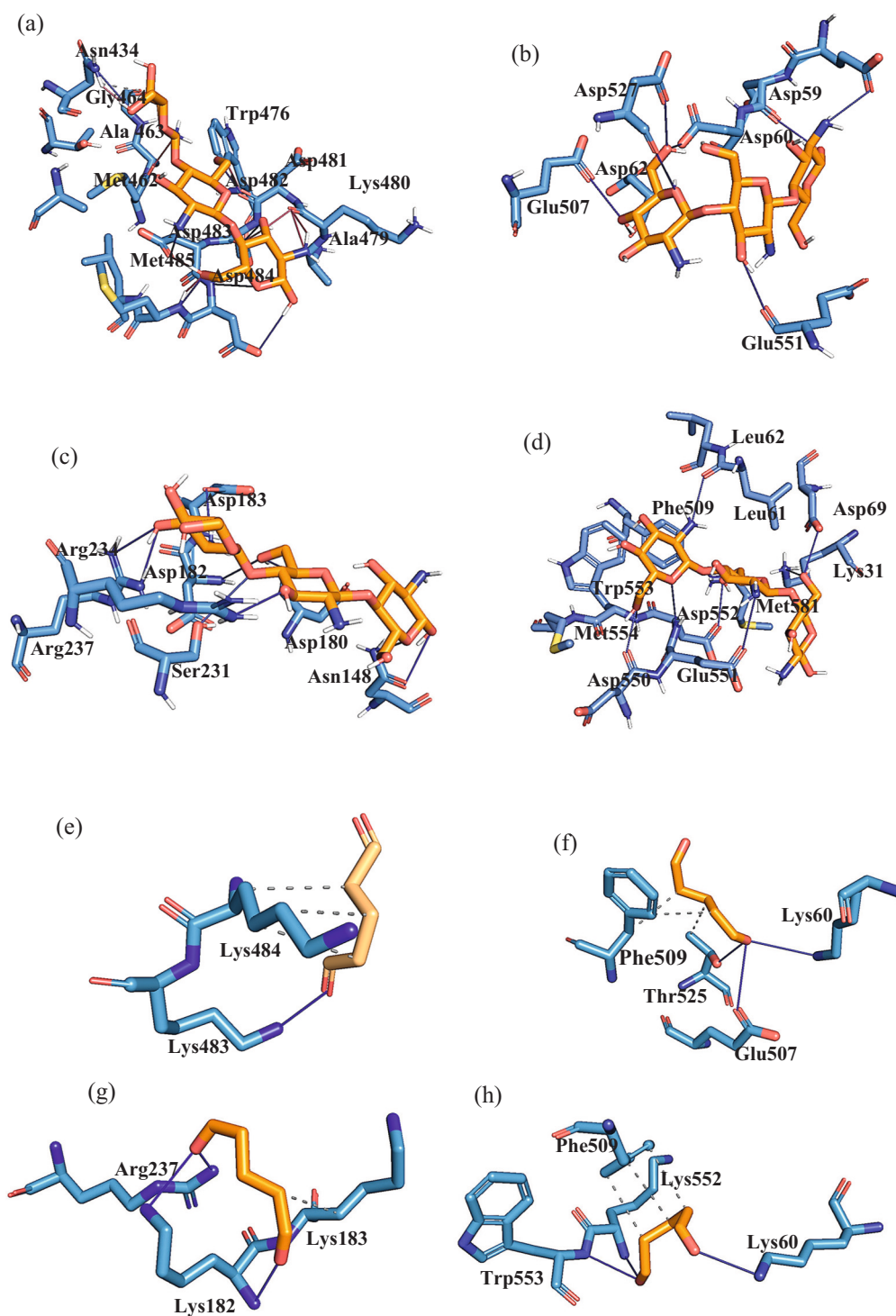


**Fig. 8.** Intermolecular interactions of crosslinkers and Mag1 variants. (a) Mag1-mDc and chitosan, (b) Mag1-mDs and chitosan, (c) Mag1-mDh and chitosan, (d) Mag1-mDr and chitosan, (e) Mag1-mKc and glutaraldehyde, (f) Mag1-mKs and glutaraldehyde, (g) Mag1-mKh and glutaraldehyde and (h) Mag1-mKr and glutaraldehyde. Cross-linker is displayed in orange whilst enzyme is in blue. (For interpretation of the references to colour in this figure legend, the reader is referred to the web version of this article.)

have larger aggregate size than that of Mag1-CLEAs and this is confirmed by particle size analysis (Supplementary 4).

It was also noted that mutant-CLEAs have a more irregular (less organised) shape aggregates than that of Mag1-CLEAs and many studies have reported that irregular and larger shaped CLEAs may create substrate diffusion limitations and more difficulty in recovering CLEAs after reaction [4,68]. Substrate diffusion limitation can be caused by compact packing of the enzyme molecules whilst aggregating [69]. The mechanistic activity of an immobilised enzyme is influenced by the pore volume and diameter [70,71]. However, this study showed contrasting results as per discussed in above sections. This could be due to the

increase formation of enzyme aggregates that occur after the establishment of additional cross-linking interactions on variant-CLEAs [12]. Additionally, the structure of variant-CLEAs with substitution at  $\alpha$ -helix and  $\beta$ -sheet were shown to have more cavities than CLEAs with substitution at coil and random sites. The increasing number of cavities in Mag1-mDh-, Mag1-mKh-, Mag1-mDs- and Mag1-mKs-CLEAs is because more cross-linkers are able to interact with the enzymes [72] in a more oriented conformation ( $\alpha$ -helix and  $\beta$ -sheets regions), thus creating a larger surface area for better mass transfer. The presence of more cavities on the structure could be the reason for better substrate accessibility to the catalytic region of CLEAs particles, therefore validating the

kinetics performance of variant-CLEAs.

### 3.6. CLEAs functional groups composition analysis

Functional groups compositions of Mag1- and variant-Asp-CLEAs were determined by using FTIR (Fig. 7). Major peaks in the IR spectra appeared in two regions, 3300–2700  $\text{cm}^{-1}$  and 1480–1200  $\text{cm}^{-1}$ . The area 3300–2700  $\text{cm}^{-1}$  correlates with N–H and O–H stretching associated with intra- and inter-molecular bound hydroxyl groups interactions [73] and peaks in the range of 1400–1200  $\text{cm}^{-1}$  were attributed to C–N stretching and N–H bending of amide II and amide III [74]. Prominent and more intense peaks were observed in all variant-CLEAs indicating increased formation of those linkages after the cross-linking process. Lys-variant-CLEAs exhibited similar profile as mutants-Asp-CLEAs (data not shown).

### 3.7. CLEAs interactions through *in silico* analysis

The improved properties and activities of Mag1 variants CLEAs are believed to be caused by an increase in interactions between cross-linkers and enzyme. In order to understand the effect of mutagenesis on the interactions of enzyme-CLEAs, docking and molecular dynamics simulations were performed on Mag1 variants and cross-linkers (glutaraldehyde or chitosan).

It was observed that chitosan formed intermolecular interactions with Asp on the surface of Mag1 variants (Fig. 8a–d). Bonds were established between the functional group of chitosan and -COOH group of substituted Asp in Mag1-mDc (Asp481, Asp482 and Asp484), Mag1-mDr (Asp550 and Asp552), Mag1-mDs (Asp59, Asp60 and Asp62) and Mag1-mDh (Asp183). Meanwhile, tethering sites between glutaraldehyde and substituted Lys on Mag1-mKs, Mag1-mKc, Mag1-mKr and Mag1-mKh were at Lys60, Lys484, Lys552 and Lys183, respectively (Fig. 7e–h) showed that the functional group of glutaraldehyde (-OH) interacts with -NH<sub>2</sub> group of Lys to establish covalent binding. Other than that, both cross-linkers also formed other interactions such as hydrophobic interactions and hydrogen bonds with the enzymes.

Due to the aggregates particles of CLEAs, it is difficult to observe or characterise the real conformation or orientation of the immobilised enzymes (Supplementary 5). Nonetheless, increasing the establishment of covalent bonding ensures the increase of the strength of immobilised particles, hence enhancing the properties and operational stability of the biocatalysts [75]. According to Wu et al. (2015) [76] site-specific immobilisation could also increase solvation of hydrophobic groups and promote enzyme hydration, thus leading to higher substrate diffusion. Through chemistry coordination between the exposed functional group of residues and cross-linkers, one immobilised orientation will prevail over the other [63]. This could be the reason why surface modification on  $\alpha$ -helix and  $\beta$ -sheets fared better in terms of enzyme performance compared to coil and random modifications.

## 4. Conclusions

In this work, the development of non-carrier enzyme immobilisation through the combination of *in silico* analysis and protein engineering has produced stable, ecological and enzymatically active biocatalysts. The utilisation of molecular docking and molecular dynamics simulation of cross-linkers (glutaraldehyde or chitosan) interacting with Mag1 has led to the designation of variation of mutants with site-specific alteration without the loss of structure architecture. Surface modification to lysine (preferred by glutaraldehyde) and aspartic acid (preferred by chitosan) has increased and strengthened the intermolecular interactions between the enzyme and cross-linker, thus, improving enzyme stability and recyclability properties compared to Mag1-CLEAs. In addition, modification on defined secondary structures (Mag1-mDh, Mag1-mDs, Mag1-mKh and Mag1-mKs) exhibited higher recovery activity compared to random and coil structures hence verifying that different orientations of

tethering sites are also responsible for the different behaviour and stability of the immobilised enzymes. The trade-off between stability and activity was demonstrated where it was shown that free enzyme activity is higher in comparison to the immobilised enzymes whilst the stability of enzyme-CLEAs is higher compared to soluble enzymes. However, since CLEAs properties allow continuous production of products (up to 8 cycles), this far outweighs the disadvantages arising from the reduction in the enzyme activity. Improved stability is vital for developing economically competitive biocatalysts with recoverable and recyclable properties. Taken together, the systematic approach of utilising computational and experimental analyses established here could potentially be used to facilitate the designing of CLEAs that maximise both activity and stability of the developed biocatalyst.

## CRedit authorship contribution statement

**Nardiah Rizwana Jaafar:** Methodology, Investigation, Formal analysis, Validation, Writing – original draft, Writing – review & editing. **Nashriq Jailani:** Methodology, Investigation. **Roshanida A. Rahman:** Conceptualization, Supervision. **Ebru Toksoy Öner:** Conceptualization, Validation, Writing – review & editing. **Abdul Munir Abdul Murad:** Conceptualization, Funding acquisition, Validation, Supervision. **Rosli Md Illias:** Conceptualization, Funding acquisition, Validation, Project administration, Supervision, Writing – original draft, Writing – review & editing.

## Declaration of competing interest

None.

## Acknowledgement

This project was financially supported by Universiti Teknologi Malaysia under the research grant Q.J130000.21A2.05E32.

## Appendix A. Supplementary data

Supplementary data to this article can be found online at <https://doi.org/10.1016/j.ijbiomac.2022.05.169>.

## References

- [1] R. Wohlgemuth, Biocatalysis – key enabling tools from biocatalytic one-step and multi-step reactions to biocatalytic total synthesis, *New Biotechnol.* 60 (2021) 113–123.
- [2] A. Madhavan, R. Sindhu, P. Binod, R.K. Sukumaran, A. Pandey, Strategies for design of improved biocatalysts for industrial applications, *Bioresour. Technol.* 245 (2017) 1304–1313.
- [3] R.A. Sheldon, *Cross-linked Enzyme Aggregates (CLEAs®): Stable and Recyclable Biocatalysts*, Press Limited, Portland, 2007.
- [4] R.A. Sheldon, Cross-linked enzyme aggregates as industrial biocatalysts, *Org. Process. Res. Dev.* 15 (2010) 213–223.
- [5] M. Ghiaci, H. Aghaei, S. Soleimani, M.E. Sedaghat, Enzyme immobilization: part 1. Modified bentonite as a new and efficient support for immobilization of *Candida rugosa* lipase, *Appl. Clay Sci.* 43 (2009) 289–295.
- [6] M.K. Nezhad, H. Aghaei, Tosylated cloisite as a new heterofunctional carrier for covalent immobilization of lipase and its utilization for production of biodiesel from waste frying oil, *Renew. Energy* 164 (2021) 876–888.
- [7] H. Aghaei, A. Yasinian, A. Taghizadeh, Covalent immobilization of lipase from *Candida rugosa* on epoxy-activated cloisite 30B as a new heterofunctional carrier and its application in the synthesis of banana flavor and production of biodiesel, *Int. J. Biol. Macromol.* 178 (2021) 569–579.
- [8] S. Aggarwal, A. Chakravarty, S. Ikram, A comprehensive review on incredible renewable carriers as promising platforms for enzyme immobilization and thereof strategies, *Int. J. Biol. Macromol.* 167 (2021) 962–986.
- [9] R.A. Sheldon, Characteristic features and biotechnological applications of crosslinked enzyme aggregates (CLEAs), *Appl. Microbiol. Biotechnol.* 92 (2011) 467–477.
- [10] J.D. Cui, L.L. Li, Y.M. Zhao, Simple technique for preparing stable and recyclable cross-linked enzyme aggregates with crude-pored microspherical silica core, *Ind. Eng. Chem. Res.* 53 (2014) 16176–16182.
- [11] N.N. Nawawi, Z. Hashim, N.H.A. Manas, N.I.W. Azelee, R.M. Illias, A porous-cross linked enzyme aggregates of maltogenic amylase from *Bacillus licheniformis* G1: robust

- biocatalyst with improved stability and substrate diffusion, *Int. J. Biol. Macromol.* 148 (2020) 1222–1231.
- [12] N.H. Abd Rahman, N.R. Jaafar, N.A. Shamsul Annuar, R.A. Rahman, A.M. A. Murad, R.M. Illias, Efficient substrate accessibility by cross-linked enzyme aggregates of levanase using dialdehyde starch-tapioca as a cross-linker, *Carbohydr. Polym.* 267 (2021), 118159.
- [13] J. Zdarata, T. Machalowski, O. Degorska, K. Bachosz, A. Fursov, H. Ehrlich, V. N. Ivaneko, T. Jesionowski, 3D chitin scaffolds from the marine demosponge *Aplysina archeri* as a support for laccase immobilization and its use in the removal of pharmaceuticals, *Biomolecules* 10 (2020).
- [14] W. Qiao, Z. Zhang, Y. Qian, L. Xu, H. Guo, Bacterial laccase immobilised on a magnetic dialdehyde cellulose without cross-linking agents for decolorization, *Colloids Surf. A Physicochem. Eng. Asp.* 632 (2022), 127818.
- [15] K. Saikia, A.K. Rathankumar, V.K. Vaithyanathan, H. Cabana, V.K. Vaidyanathan, Preparation of highly diffusible porous cross-linked lipase B from *Candida antarctica* conjugates: advances in mass transfer and application in transesterification of 5-hydroxymethylfurfural, *Macromolecules* 170 (2021) 583–592.
- [16] M. Primožič, G. Kravanja, Z. Knez, A. Crnjac, M. Leitgeb, Immobilized laccase in the form of (magnetic) cross-linked enzyme aggregates for sustainable diclofenac (bio)degradation, *J. Clean. Prod.* 275 (2020), 124121.
- [17] S. Hero, A.H. Morales, N.I. Perotti, C.M. Romero, M.A. Martinez, Improved development on magnetic xyl-CLEAs technology for biotransformation of agro-industrial by-products through the use of a novel macromolecular cross-linker, *React. Funct. Polym.* 154 (2020), 104676.
- [18] R.A. Sheldon, A. Basso, D. Brady, New frontiers in enzyme immobilisation: robust biocatalysts for a circular bio-based economy, *Chem. Soc. Rev.* 50 (2021) 5850–5862, 101039/d1cs00015b.
- [19] C. Ottone, O. Romero, P. Urrutia, C. Bernal, A. Illanes, L. Wilson, Enzyme biocatalysis and sustainability, in: M. Piumetti, S. Benaid (Eds.), *Nanostructured Catalysts for Environmental Applications*, Springer, Cham, 2021, [https://doi.org/10.1007/978-3-030-58934-9\\_14](https://doi.org/10.1007/978-3-030-58934-9_14).
- [20] K. Sellami, A. Couvert, N. Nasrallah, R. Maachi, N. Tandjaoui, M. Aouseoud, A. Amrane, Bio-based and cost effective method for phenolic compounds removal using cross-linked enzyme aggregates, *J. Hazard. Mater.* 403 (2021), 124021.
- [21] R.C. Rodrigues, O. Barbosa, C. Ortiz, A. Berenguer-Murcia, R. Torres, R. Fernandez-Lafuente, Amination of enzymes to improve biocatalyst performance: coupling genetic modification and physicochemical tools, *RSC Adv.* 4 (2014) 38350–38374.
- [22] B. Wei, F. Liu, X. Liu, L. Heng, Q. Yuan, H. Gao, H. Liang, Enhancing stability and by-product tolerance of  $\beta$ -glucuronidase based on magnetic cross-linked enzyme aggregates, *Colloid Surf. B: Biointerfaces* 210 (2022), 112241.
- [23] T.L. Ogorzalek, S. Wei, Y. Liu, Q. Wang, C.L. Brooks, Z. Chen, E.N.G. Marsh, Molecular-level insights into orientation-dependent changes in the thermal stability of enzymes covalently immobilized on surfaces, *Langmuir* 31 (22) (2015) 6145–6153.
- [24] C. Bernal, K. Rodríguez, R. Martínez, Integrating enzyme immobilization and protein engineering: an alternative path for the development of novel and improved industrial biocatalysts, *Biotechnol. Adv.* 36 (5) (2018) 1470–1480.
- [25] K. Rodríguez-Núñez, C. Bernal, R. Martínez, Immobilized biocatalyst engineering: high throughput enzyme immobilization for the integration of biocatalyst improvement strategies, *Int. J. Biol. Macromol.* 170 (2021) 61–70.
- [26] H. Guterres, S.J. Park, W. Jiang, W. Im, Ligand binding site refinement to generate reliable holo protein structure conformations from apo structures, *J. Chem. Inf. Model.* 61 (1) (2021) 535–546.
- [27] P.G. Chandler, S.S. Broendum, B.T. Riley, M.A. Spence, C.J. Jackson, S. McGowan, A.M. Buckle, Strategies for increasing protein stability, *Methods Mol. Biol.* 2073 (2020) 163–181.
- [28] S.K. Sinha, S. Das, S. Konar, P.K. Ghorai, R. Das, S. Datta, Elucidation the regulation of glucose tolerance in a  $\beta$ -glucosidase from halothermothrix orenii by active site pocket engineering and computational analysis, *Int. J. Biol. Macromol.* 156 (2020) 621–632.
- [29] C. Chen, M.C. Melo, A. Khan, C. la Fuente-Nunez, J.P. Imschneider, M. B. Imscheider, Understanding and modelling the interactions of peptides with membranes: from partitioning to self-assembly, *Curr. Opin. Struct. Biol.* 61 (2020) 160–166.
- [30] M.K.H. Abdul Wahab, H.A. El-Enshasy, F.D. Abu Bakar, A.M.A. Murad, J.M. Jahim, R.M. Illias, Improvement of cross-linking and stability on cross-linked enzyme aggregate (CLEA)-xylanase by protein surface engineering, *Process Biochem.* 86 (2019) 40–49.
- [31] H. Aghaei, Z. Mohammadbagheri, A. Hemasi, A. Taghizadeh, Efficient hydrolysis of starch by  $\alpha$ -amylase immobilized on cloisite 30B and modified forms of cloisite 30B by adsorption and covalent methods, *Food Chem.* 373 (2022), 131425.
- [32] S. Mortazavi, H. Aghaei, Make proper surfaces for immobilization of enzymes: immobilization of lipase and  $\alpha$ -amylase on modified na-sepiolite, *Int. J. Biol. Macromol.* 164 (2020) 1–12.
- [33] Š. Janěček, F. Marěček, E.A. MacGregor, B. Svensson, Starch-binding domains as CBM families—history, occurrence, structure, function and evolution, *Biotechnol. Adv.* 37 (2019), 107451.
- [34] A.L.O. Gaenssle, H.H.M. Bax, E.C. van der Maarel, E. Jurak, GH13 glycogen branching enzymes can adapt the substrate chain length towards their preferences via  $\alpha$ -1,4-transglycosylation, *Enzyme Microbiol. Technol.* 150 (2021), 109882.
- [35] N. Eswar, B. Webb, M.A. Marti-Renom, M.S. Madhusudhan, D. Eramian, M.Y. Shen, Comparative protein structure modelling using MODELLER, *Curr. Protoc. Protein Sci.* 2 (2007) 2–9.
- [36] N.H. Abdul Manas, F.D. Abu Bakar, R.M. Illias, Computational docking, molecular dynamics simulation and subsite structure analysis of a maltogenic amylase from *Bacillus lehensis* G1 provide insights into substrate and product specificity, *J. Mol. Graph. Model.* 67 (2016) 1–13.
- [37] O. Trott, A.J. Olson, Autodock Vina: improving the speed and accuracy of docking with a new scoring function, efficient optimization and multi-threading, *J. Comput. Chem.* 31 (2010) 455–461.
- [38] S. Kim, J. Chen, T. Cheng, A. Gindulyte, J. He, S. He, Q. Li, B.A. Shoemaker, P. A. Thiessen, B. Yu, L. Zaslavsky, J. Zhang, E.E. Bolton, PubChem in 2021: new data content and improved web interfaces, *Nucleic Acids Res.* 49 (1) (2019) 1388–1395.
- [39] M.J. Abraham, T. Murtola, R. Schulz, S. Páll, J.C. Smith, B. Hess, E. Lindahl, GROMACS: high performance molecular simulations through multi-level parallelism from laptops to supercomputers, *SoftwareX* 1–2 (2015) 19–25.
- [40] A. Bordat, M.-C. Houvenaghel, S. German-Retana, Gibson assembly: an easy way to clone plasmid full-length infectious cDNA clones expressing an ectopic VPg, *Virology* 533 (2015) 89.
- [41] N.H. Abdul Manas, S. Pachelles, N.M. Mahadi, R.M. Illias, The characterisation of an alkali-stable maltogenic amylase from *Bacillus lehensis* G1 and improved maltotriose production by hydrolysis suppression, *PLoS ONE* 9 (9) (2014).
- [42] Y. Fu, J. Zhao, Z. Chen, Insights into the molecular mechanisms of protein-ligand interactions by molecular docking and molecular dynamics simulation: a case of oligopeptide binding protein, *Comput. Math. Methods Med.* 2018 (2018), 3502514.
- [43] E.S. Redeker, D.T. Ta, D. Cortens, B. Billen, W. Guedens, P. Adriaensens, Protein engineering for directed immobilization, *Bioconjug. Chem.* 24 (2013) 1761–1777.
- [44] J. Liu, B. Wei, C. Che, Z. Gong, Y. Jiang, M. Si, Z. Junming, G. Yang, Enhanced stability of manganese superoxide dismutase by amino acid replacement designed via molecular dynamics simulation, *Int. J. Biol. Macromol.* 128 (2019) 297–303.
- [45] Y. Liu, T.L. Ogorzalek, P. Yang, M.M. Schroeder, E.N.G. Marsh, Z. Chen, Molecular orientation of enzymes attached to surfaces through defined chemical linkages at the solid-liquid interface, *J. Am. Chem. Soc.* 135 (3) (2013) 12660–12669.
- [46] A.J. Pineda-Knauseder, D.A. Vargas, R. Fasan, Organic solvent stability and long-term storage of myoglobin-based carbene transfer biocatalysts, *Biotechnol. Appl. Biochem.* 67 (2020) 516–526.
- [47] W. Abdallah, X. Hong, S. Banta, I. Wheeldon, Microenvironmental effects can masquerade as substrate channelling in cascade biocatalysis, *Curr. Opin. Biotechnol.* 73 (2022) 233–239.
- [48] Y. Gao, C.C. Roberts, J. Zhu, J.-L. Lin, C.A. Chang, I. Wheeldon, Tuning enzyme kinetics through designed intermolecular interactions far from the active site, *ACS Catal.* 5 (2015) 2149–2153.
- [49] M. Kubiak, I. Kampen, C. Schilde, C. Structure-based modeling of the mechanical behavior of cross-linked enzyme crystals, *Crystals* 12 (2022) 441.
- [50] R.S. Singh, T. Singh, Glutaraldehyde functionalization of halloysite nanoclay enhances immobilization efficacy of endonuclease for fructooligosaccharides production from inulin, *Food Chem.* 381 (2022), 132253.
- [51] T. Jiang, R. James, J.S. Kumber, C.T. Laurencin, Chitosan as a biomaterials: structure, properties and applications in tissue engineering and drug delivery, *Nat. Synth. Biomed. Polym.* (2014) 91–113.
- [52] O. Barbosa, C. Ortiz, A. Berenguer-Murcia, R. Torres, R.C. Rodrigues, R. Fernandez-Lafuente, Glutaraldehyde in bio-catalysts design: a useful crosslinker and a versatile tool in enzyme immobilization, *RCS Adv.* 4 (2014) 1583–1600.
- [53] E. Szymańska, K. Winnicka, Stability of chitosan—a challenge for pharmaceutical and biomedical applications, *Mar. Drugs* 13 (2015) 1819–1846.
- [54] F. Liu, W. Chang, M. Chen, F. Xu, J. Ma, F. Zhong, Tailoring physicochemical properties of chitosan and their protective effects on meat by varying drying temperature, *Carbohydr. Polym.* 212 (2019) 150–159.
- [55] A. Matei, C. Puscas, I. Patrascu, M. Lehene, J. Ziebro, F. Scurtu, M. Baia, D. Porumb, R. Totos, R. Solaghi-Dumitruc, Stability of glutaraldehyde in biocide compositions, *Int. J. Mol. Sci.* 21 (2020) 3372.
- [56] J. Feng, S. Yu, J. Li, T. Mo, P. Li, Enhancement of the catalytic activity and stability of immobilized aminoacylase using modified magnetic Fe<sub>3</sub>O<sub>4</sub> nanoparticles, *Chem. Eng. J.* 286 (2016) 216–222.
- [57] S. Parveen, M. Asgher, M. Bilal, Lignin peroxidase-based cross-linked enzyme aggregates (Lip-CLEAs) as robust biocatalytic materials for mitigation of textile dyes-contaminated aqueous solution, *Environ. Technol. Innov.* 21 (2021), 101226.
- [58] F. Rusmini, Z. Zhong, J. Feijen, Protein immobilization strategies for protein biochips, *Biomacromolecules* 8 (2007) 1775–1789.
- [59] C.D.-O.C. Mateo, O. Abian, M. Bernedo, E. Cuenca, M. Fuentes, G. Fernandez-Lorenzo, J.M. Palomo, V. Grazu, B.C.C. Pessela, C. Giacomini, Some special features of glyoxyl supports to immobilize proteins, *Enzym. Microb. Technol.* 37 (2005) 456–462.
- [60] S. Ba, L. Haroune, C. Cruz-Morató, C. Jacquet, I.E. Touhar, J.-P. Bellenger, C. Y. Legault, P. Jones, H. Cabana, Synthesis and characterization of combined cross-linked laccase and tyrosinase aggregates transforming acetaminophen as a model phenolic compound in wastewaters, *Sci. Total Environ.* 487 (15) (2014) 747–755.
- [61] J.M. Bolivar, B. Nidetzky, The microenvironment in immobilized enzymes: methods of characterization and its role in determining enzyme performance, *Molecules* 24 (2019) 3460.
- [62] X. Zou, S. Wei, S. Badieyan, M. Schroeder, J. Jasensky, C.L. Brooks, E.N.G. Marsh, Z. Chen, Investigating the effect of two-point surface attachment on enzyme stability and activity, *J. Am. Chem. Soc.* 140 (48) (2018) 16560–16569.
- [63] Y. Li, T.L. Ogorzalek, S. Wei, X. Zhang, P. Yang, J. Jasensky, C.L. Brooks, E.N.G. Marsh, Z. Chen, Effect of immobilization site on the orientation and activity of surface-tethered enzymes, *Phys. Chem.* 20 (2018) 1021–1029.
- [64] K.A. Wildman, D.-K. Lee, A. Ramamoorthy, Determination of  $\alpha$ -helix and  $\beta$ -sheet stability in the solid state: a solid-state NMR investigation of poly(L-alanine), *Biopolymers* 64 (2002) 246–254.

- [65] S. Mortazavi, H. Aghaei, Make a proper surfaces for immobilization of enzymes: immobilization of lipase and  $\alpha$ -amylase on odified na-sepiolite, *Int. J. Biol. Macromol.* 164 (2020) 1–12.
- [66] H. Aghaei, M. Ghavi, G. Hashemkhani, M. Keshavarz, Utilization of two modified layered doubled hydroxides as supports for immobilization of *Candida rugosa* lipase, *Int. J. Biol. Macromol.* 162 (2020) 74–83.
- [67] S.L. Hosseinipour, M.S. Khiabani, H. Hamishehkar, R. Salehi, Enhanced stability and catalytic activity of immobilized  $\alpha$ -amylase on modified Fe<sub>3</sub>O<sub>4</sub> nanoparticles for potential application in food industries, *J. Nanopart. Res.* 17 (2015) 382.
- [68] L.T. Nguyen, N. Seow, K.-L. Yang, Hollow cross-linked enzyme aggregates (h-CLEAs) of laccase with high uniformity and activity, *Colloids Surf. B: Biointerfaces* 151 (2016) 88–94.
- [69] R. Schoevaart, M.W. Wolbers, M. Golubovic, M. Ottens, A.P.G. Kieboom, F. van Rantwijk, L.A.M. van der Wielen, R.A. Sheldon, Preparation, optimization, and structures of cross-linked enzyme aggregated (CLEAs), *Biotechnol. Bioeng.* 87 (2004) 754–762.
- [70] M. Ghiaci, H. Aghaei, S. Soleimani, M.E. Sedaghat, Enzyme immobilization: part 2: immobilization of alkaline phosphatase on na-bentonite and modified bentonite, *Appl. Clay Sci.* 43 (2009) 308–316.
- [71] M.E. Sedaghat, M. Ghiaci, H. Aghaei, S. Soleimani-Zad, Enzyme immobilization. Part 4. Immobilization of alkaline phosphatase on na-sepiolite and modified sepiolite, *Appl. Clay Sci.* 46 (2009) 131–135.
- [72] F. Šulek, D.P. Fernández, Ž. Knez, M. Habulin, R.A. Sheldon, Immobilization of horseradish peroxidase as crosslinked enzyme aggregates (CLEAs), *Proc. Biochem.* 46 (3) (2011) 765–769.
- [73] C. Pan, J. Qian, C. Zhao, H. Yang, X. Zhao, H. Guo, Study on the relationship between crosslinking degree and properties of TPP crosslinked chitosan nanoparticles, *Carbohydr. Polym.* 241 (2020), 116349.
- [74] J. Kong, S. Yu, Fourier transform infrared spectroscopic analysis of protein secondary structures, *Acta Biochim. Biophys. Sin.* 39 (8) (2007) 549–559.
- [75] P. Zucca, E. Sanjust, Inorganic materials as support for covalent enzyme immobilization: methods and mechanisms, *Molecules* 19 (2014) 14139–14194.
- [76] Z. Wu, P. Yang, Simple multipurpose surface functionalization by phase transited protein adhesion, *Adv. Mater. Interfaces* 2 (2) (2014), 1400401.